SEISMIC BEHAVIORS OF ECC/CONCRETE COMPOSITE BEAM-COLUMN JOINTS UNDER REVERSED CYCLIC LOADING

J.L. PAN[*] F. YUAN[*]

* Key Laboratory of Concrete and Prestressed Concrete Structures of Ministry of Education
School of Civil Engineering, Southeast University, Nanjing, China
e-mail: jinlongp@gmail.com

†Key Laboratory of Concrete and Prestressed Concrete Structures of Ministry of Education
School of Civil Engineering, Southeast University, Nanjing, China
e-mail: yf_1542@163.com

Key words: Ductility, Multiple cracking, Beam-column Joints, Seismic resistance

Abstract: Engineered cementitious composites (ECC) are a class of high-performance fiber reinforced cement composite with strain hardening and multiple cracking properties. In this paper, a number of RC/ECC composite beam-column joints have been tested under reversed cyclic loading to study the effect of substitution of concrete with ECC in the joint zone on the seismic behaviors of composite members. The experimental parameters include shear reinforcement ratio in the joint zone, axial load level on the column and substitution of concrete with ECC or not. According to the test results, for the specimens without shear reinforcement ratio in the joint zone, substitution of concrete with ECC in the joint zone cannot change the brittle shear failure in the joint zone, but can significantly increase the load capacity and ductility of the beam-column joint specimens, as well as the energy dissipation ability. For the specimens with insufficient or proper shear reinforcement ratio, application of ECC in the joint zone can lead to failure mode change from brittle shear failure in the joint zone to a more ductile failure mode, i.e. flexural failure at the base of the beam, with increased load capacity, ductility and energy dissipation ability. Increase of axial load on column and shear reinforcement in the joint zone have little effect on seismic behaviors of the members since they all failed by flexural failure at the base of beam. In a word, the substitution of concrete with ECC in the joint zone was experimentally proved to be an effect method to increase the seismic resistance of beam-column joint specimens.

1 INTRODUCTION

For conventional reinforced concrete frame structures, the seismic performance mostly depends on the deformation ability of key components such as beams, columns and their joint zones. Under earthquake actions, these members are expected to maintain substantial inelastic deformations without a significant loss of load carrying capacity. Among these structural components, beam-column joints are designed to sustain vertical live or dead loads transferred from beams and slabs, horizontal loads from earthquake actions and wind, leading to complicated stresses in the joint zone, as shown in Fig. 1. Evidence from recent earthquakes showed beam-column joints with insufficient transverse steel reinforcement often failed by brittle shear failure with ‘x’ shape cracks under reversed cyclic loading during the earthquake. Once brittle shear failure in the joint zones occurs, the joint cannot sustain any external and internal loading and maintain integrity of the frame structure, indicating that final failure of the frame structure is reached [1]. To increase

seismic performance of frame structures, the joint zones are reinforced with additional transverse steel reinforcement, which serve as confinement of the concrete core and lead to enhancement of shear capacity in the joint zone. Meanwhile, premature buckling of longitudinal steel reinforcement can be avoided by the confining effect of the transverse steel reinforcement [2]. With additional transverse steel reinforcement, brittle shear failure can be avoided in the joint zone with a significant increase of structural ductility and seismic resistance. However, on the other hand, an increased amount of transverse steel reinforcement in the joint zone will also bring forth two aspects of problems. Dense shear reinforcement ratio may lead to difficulties in placing steel bars because of space limitation, and the compactness of concrete cannot be guaranteed, leading to more defects in the joint zone. For reinforced concrete structures, another intrinsic deficiency is the brittleness of concrete especially in tension or shear. For concrete frame structures, seismic cyclic loading always leads to concrete spalling, bond splitting, brittle shear failure in the joint zone. Though transverse steel reinforcement can provide composite action with concrete and achieve a virtually ductile deformation behavior, the inherent brittleness of concrete cannot be modified and the deficiency with respect to steel/concrete interaction, interfacial bond deterioration, and composite integrity are still challenges for conventional reinforced concrete. Incompatible deformation between concrete and steel reinforcement can decrease interfacial slip, bond deterioration, resulting in decreased deformation ability and load capacity of concrete members.

In recent years, a class of high performance fiber reinforced cementitious composites (called engineered cementitious composites (ECC) with ultra ductility, has been developed for applications in construction industry [3-5]. Substitution of conventional concrete with ECC strategically in concrete frame structures may provide a method to solve the deficiencies resulting from brittleness of concrete. ECC and concrete have similar range of tensile (4-6 MPa) and compressive strengths (30-80 MPa), while they have distinctly difference in tensile deformation behaviour. For conventional concrete, it fails in a brittle manner once its tensile strength is reached. However, for an ECC plate under uniaxial tension, after first cracking, tensile load capacity continues to increase with strain hardening behavior accompanied by multiple cracks along the plate. Typically, mechanical softening of ECC starts at a tensile strain of 3-5%, with a crack spacing of 3-6 mm and crack width of about 60 μm [6]. In compression, ECC has the similar strength as concrete with increased strain at the ultimate strength, resulting in a lower elastic stiffness compared with concrete due to lack of coarse aggregate. After the peak stress, the compressive stress drops to 0.5fc and followed by descending stress with further increasing compression deformation [7]. Existing research indicated that the mechanical properties of ECC material in shear are similar to those in tension [8]. The enhanced shear capacity and ductility provide an alternative way to increase the shear resistance and ductility of reinforced concrete members.

Previous study indicated that the combination of ECC and steel reinforcement can lead to compatible deformation in uniaxial tension, resulting in decreased interfacial bond stresses and elimination of bond splitting cracks and cover splitting [9]. ECC beams without transverse steel reinforcement demonstrated superior mechanical performance to concrete beams with closely spaced stirrups, indicating that elimination of shear reinforcement is feasible when concrete was replaced by ECC [10]. Experiments on the cyclic response of steel reinforced ECC columns [11] and frames [12] also confirmed that the structure integrity could be maintained better when concrete was replaced by ECC. For reinforced concrete frame structures, it is vital to avoid brittle shear failure in critical components such as columns and beam-column joints. Substitution of concrete with ductile ECC in the joint zone and the end zones of beams and columns are also expected to obtain compatible deformation between ECC and longitudinal steel reinforcement

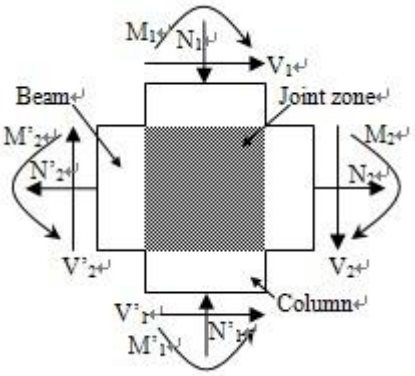

Fig 1 : External forces applied on a beam-column joint

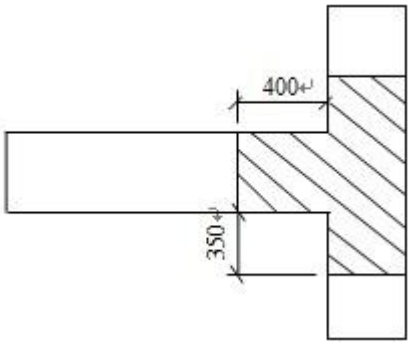

Fig 2: Part made with ECC for RC/ECC joint specimens

especially in inelastic deformation regime, resulting in increased load capacity, ductility and energy dissipation. With higher shear strength, ECC materials in the joint zones or outside can decrease the amount of transverse steel reinforcement in these regimes. Moreover, the confinement effect of ECC together with that from transverse shear reinforcement can avoid buckling of longitudinal steel reinforcement and maintain composite integrity, and a ductile failure can be guaranteed. Though ECC itself is unable to recover the energy dissipation capacity under reversed cyclic loading, the stabilizing effect from strategically application of ECC on the longitudinal reinforcement and damage tolerance at large deformation can considerably increase the seismic performance of reinforcement concrete structures.

In this paper, structural behaviours of beam-column joints with application of ECC in the joint zone were investigated and compared with conventional reinforced concrete beam-column joint specimens. The influence of different parameters, including transverse steel reinforcement ratio in the joint zone, axial load level on the column, usage of ECC in the joint zone or not, on the ultimate strength, rigidity, and energy dissipation ability, etc., are evaluated.

2 EXPERIMENTAL PROGRAM

2.1 Preparation of specimens

Due to higher cost of PVA-ECC compared with normal commercial concrete [13], application of ECC for a whole structure is essentially uneconomic. For a concrete frame structure, ECC can be utilized in some key positions for improving the seismic resistance of the structure. In this experimental study, ECC is only involved in the connection zone of the beam and column, as shown in Fig. 2.

In this experimental study, four RC/ECC composite beam-column joints and two reinforced concrete beam-column joints were tested. These joint specimens are all ‘T’ type joints for simulating the edge beam-column joints in the frame structures. For the joint specimens, the experimental parameters include application of ECC in the joint zone or not, transverse steel reinforcement ratio (0, 0.69% and 1.04%) in the joint zone, axial load level on the column, etc. Totally, four different specimen configurations are designed in this experimental study. Specimen S1 and S2 are normal reinforced concrete beam-column joint without stirrup and with two stirrups in the joint zone, and specimen S3 and S4 are ECC/RC composite beam-column joints without stirrup and with two stirrups in the joint zone, respectively. The transverse steel reinforcement in specimen S5 is the same as specimen S4 but with higher axial load on the column, while the specimen S6 is an ECC/RC composite joint with increased transverse steel reinforcement (three stirrups) in the joint zone. Table 1 gives the details of each specimen. Two levels of axial loads (350 kN and 525 kN, corresponding to 20% and 30% of the load carrying capacity of the column) were applied on the top of columns when the joint specimens were cyclically loaded in horizontal direction. The longitudinal reinforcement ratio of column and beam is 1.44% and 1.88%,

Table 1: Summary of specimen information

Specimen	Composite	$\rho_{transverse}$* (%)	Axial Load (kN)	Yielding Load		Ultimate Load		Failure Load		Ductility coefficient
				P_y kN	Δ_y mm	P_{max} kN	Δ_{max} mm	P_u kN	Δ_u mm	
S1	RC	0	350	75.3	16.2	102.4	37.8	87.0	47.9	2.96
S2	R/C	0.69	350	80.2	15.3	107.0	47.3	90.9	64.8	4.25
S3	RC/ECC	0	350	83.1	13.5	119.2	26.9	101.9	64.2	4.76
S4	RC/ECC	0.69	350	99.7	12.7	128.5	26.7	109.2	83.8	6.26
S5	RC/ECC	0.69	525	97.6	11.9	125.6	19.98	106.7	84.5	7.10
S6	RC/ECC	1.04	350	96.5	13.3	119.7	26.6	101.7	74.6	5.63

*The transverse reinforcement ratio of joints.

Table 2: Material properties of steel reinforcement

Steel type	Diameter (mm)	Yield strength fy (MPa)	Ultimate strength fu (MPa)	Modulus of elasticity Es(GPa)
mild stirrup	6	407.5	454.8	181
deformed longitudinal bar	20	359.4	541.6	187

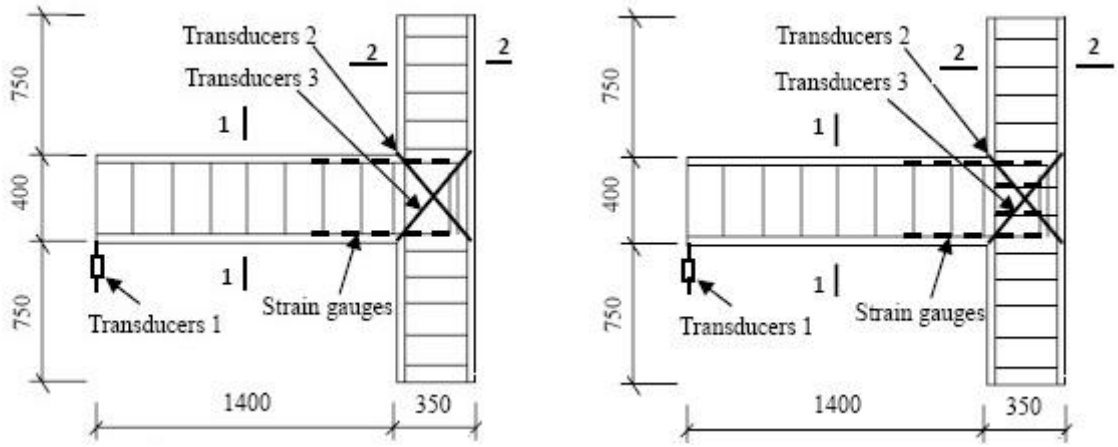

(a) for Specimens S-1, S-3 (b) for Specimens S-2, S-4, S-5, S-6

Fig 3: Details of the test joints (unit: mm)

respectively. The steel bars with the diameter of 8 mm at every 100 mm were used as shear reinforcement. The details of steel reinforcement configuration were shown in Fig. 3.

2.2 Material properties

In order to evaluate the ductility behavior of ECC used for the beam-column joints, direct tensile tests were conducted. Fig. 4 shows the

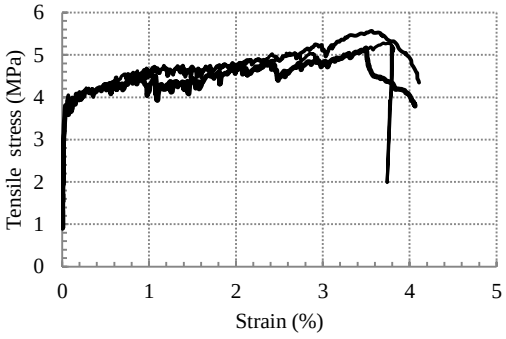

Fig 4: Tensile stress-strain relationship of ECC

tensile stress-strain curves of ECC material used for casting the beam-column joints. The test results indicated that the tensile strength exceeded 5 MPa and the ultimate tensile strain approached 4%. For the compressive strength (f_{cu}) of ECC and concrete used outside the joint zone, a number of cubic specimens with dimension of 150 mm×150 mm×150 mm were tested in compression. The compressive strength of ECC and concrete are 49.6 MPa and 52.4 MPa respectively, and the modulus of elasticity (E_c) of ECC and concrete are 34.49 GPa and 18.50 GPa respectively. Table 2 shows the measured average yield strength (f_y), tensile strength (f_u) and modulus of elasticity (E_s) for the steel reinforcement.

2.3 Loading configuration

To investigate the seismic behaviors of beam-column joints with different configurations, the tests were designed as shown in Fig. 5. The column was horizontally and simply supported on the ground with the left end leaned against the rigid reaction wall. A hydraulic jack was installed between the other end of the column and a steel frame anchored on the ground. To avoid significant displacement of the steel frame, two steel strands with high strength were tensioned and fixed on the reaction wall and the steel frame. For each specimen, the axial load was applied on the column with the hydraulic jack, and the horizontal load on the end of the beam was applied with a hydraulic actuator. The whole loading system is shown in Fig.5.

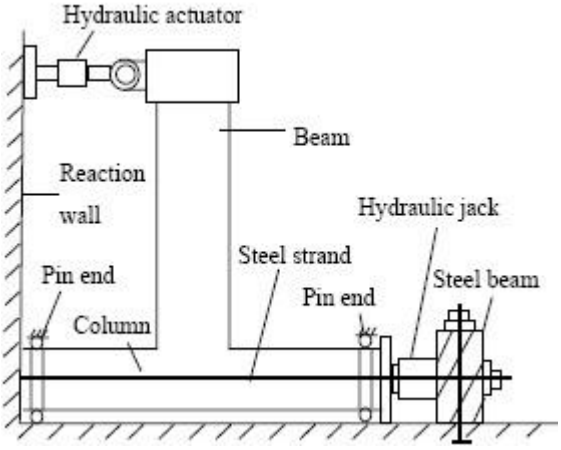

Fig 5: Test setup for all specimens

For each specimen, the loading history included elastic and inelastic cycles. The elastic cycles were conducted under load control at load levels of 0.25 P_y, 0.5 P_y and 0.75 P_y, where P_y is the estimated lateral yielding load corresponding to the lateral yielding displacement Δ_y. The load was increased at intervals of 0.05 P_y when the specimen is approaching yield strength. After yielding of the specimen occurred, inelastic cycles were conducted under displacement control at displacement levels of Δ_y, 2 Δ_y, 3 Δ_y, 4 Δ_y, 5 Δ_y and so on. Three cycles were imposed at each inelastic displacement level described above. The loading history is shown in Fig. 6. For each specimen, the test was terminated when the residual load capacity of the specimen decreased to 85% of the peak load capacity.

During the loading process, a displacement transducer was installed to obtain the displacement at the top of beam. The other two displacement transducers (LVDT) were installed to measure the shear deformation of the joint zone, as shown in Fig. 3. To measure the strain variation of the steel reinforcement, a number of strain gauges were attached on the longitudinal steel bars of the beam at a space of 80 mm within the joint zone and near the beam end, and two strain gauges were used at each side of the stirrup in the joint zone for the specimens with stirrups in the joint zone. The displacement from the LVDTs and strains from the strain gauges were automatically collected by a data logger.

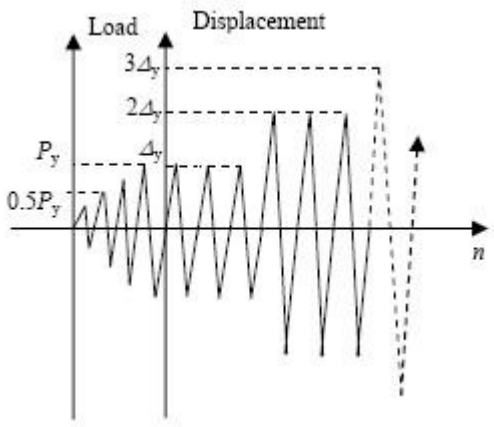

Fig 6: Cyclic loading history for each specimen

3 EXPERIMENTAL RESULTS AND DISCUSSIONS

3.1 Failure characteristics and crack patterns

For specimen S1, which is a reinforced concrete beam-column joint specimen without stirrups in the joint zone, a number of flexural cracks appeared in the height of 800 mm from the base of the beam before yielding of longitudinal steel reinforcement was reached. The cracks spacing was approximated to be 100 mm, and the cracks extended to near the center line of the beam. Diagonal cracks were observed in the joint zone. For specimen S1, steel yielding occurred at the displacement of 16.2 mm corresponding to a yield load of 75.3 kN. Beyond yielding, the cracks in the beam region kept constant while the diagonal cracks in joint zone became wider and wider. The maximum crack width observed in joint zone increased to 5 mm at the displacement of 2 Δ_y. Ultimate load capacity (102.4 kN) was obtained at the displacement of 37.8 mm. Longitudinal splitting cracks and concrete spalling were observed at the displacement of 3 Δ_y and the residual strength declined to 85% of the ultimate strength, indicating final failure was reached. S1 finally failed by brittle shear failure of concrete in joint zone, final crack pattern of specimen S1 is shown in Fig. 7.

For specimen S2, which is a normal RC beam-column joint with two stirrups in the joint zone, the failure process is most similar to the specimen S1. Before yielding occurred, a number of flexural cracks occurred in the height of 850 mm from the base of the beam. The opening and spacing of the cracks in the beam were similar to S1 while the crack width within the joint zone was much smaller than S1 due to application of stirrups. With increasing external loading, yielding occurred at the displacement of 15.3 mm with corresponding load of 80.2 kN. With further increase of the external load, the crack arising from the base of the beam increased to 7 mm at the displacement of 2 Δ_y, and more intersectional shear cracks occurred in the joint zone. When the displacement reached 3 Δ_y, localization of cracks at the height of 100 mm and 150 mm from the base of the beam occurred and connected with the cracks at the height of 300 mm and 450 mm from the other side. For these localized cracks, the crack width approached about 5 mm. With increasing displacement, more shear cracks occurred in the joint zone and localized cracks tended to open significantly to 9 mm. Meanwhile, splitting of concrete occurred at the base of the beam and within the joint zone. Finally, specimen S2 failed at a displacement of 64.8 mm (5 Δ_y) due to shear crushing of concrete in the joint zone, and final crack pattern of S2 was shown in Fig. 7.

For specimen S3, which is a RC/ECC composite beam-column joint without stirrups in the joint zone, the initial tiny crack occurred at a load of 40 kN at the interface between concrete and ECC. Prior to yielding, some tiny cracks occurred in the ECC zone of the beam, and extended to approximately 40 mm from the tension side, while larger flexural cracks formed in the beam of concrete part (400 mm to1000 mm from the base of the beam). In this stage, no cracks appeared in the joint zone. With increasing external loading, steel yielding occurred at the displacement of 13.5 mm with corresponding load of 83.1 kN. When the displacement reached 2 Δ_y, a major flexural crack appeared at the base of the beam, and some secondary cracks occurred in the joint zone. When the displacement reached 4 Δ_y, the crack at the base of the beam increased to 10 mm, and more tiny cracks occurred and formed a few intersectional shear cracks in the ECC joint zone. When the displacement reached 5 Δ_y, a major shear crack in the ECC joint zone suddenly increased to 15 mm, indicating ultimate stage of the beam-column joint specimen was reached. The corresponding ultimate load capacity was 119.2 kN. With increasing displacement, the external load decreased with the displacement, and final failure occurred at the displacement of 6 Δ_y with corresponding load of 101.9 kN. The crack patter after failure is shown in Fig. 7. Compared with specimen S1 and S2, specimen S3 showed much better ductility and higher

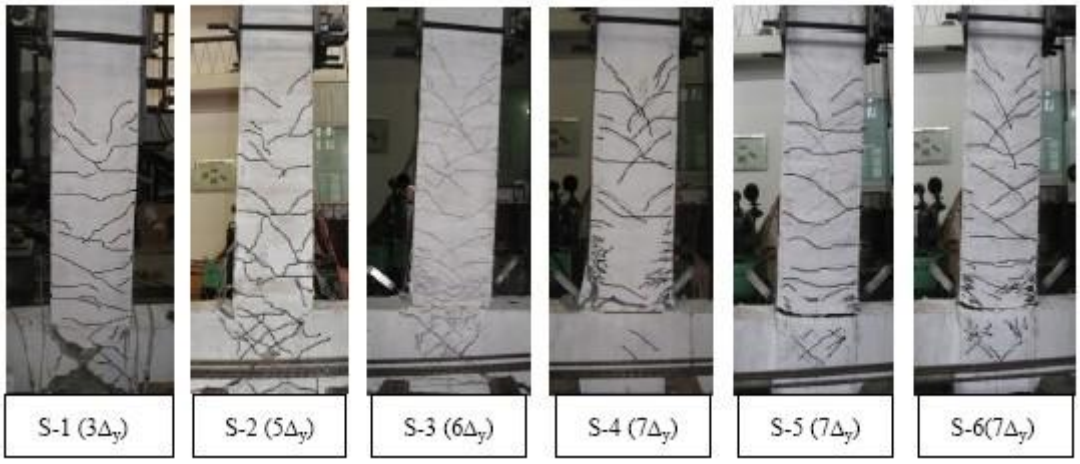

Fig 7: Crack patterns of specimens after failure

ultimate load capacity.

S4 is a RC/ECC composite beam-column joint specimen with two stirrups in the joint zone. Prior to yielding of steel reinforcement, a number of tiny flexural cracks occurred within the height of 850 mm from the base of the beam. The extension of the cracks was around 50 mm. In this stage, no cracks occurred in the joint zone. With increasing external loading, S4 reached yielding of steel reinforcement at the load value of 99.7 kN with corresponding displacement of 12.7 mm. After yielding, the joint specimen is loaded by displacement control. When the displacement reached 2 Δ_y, a major flexural crack formed at the base of the beam, and three groups of connected shear cracks formed along the beam. When the displacement reached 3 Δ_y, the crack at the base of the beam continued to open and reached about 8 mm, but the crack could not extend further along the depth of the beam and multiple tiny cracks formed near the crack tip. During increase of displacement from 4 Δ_y to 6 Δ_y, the beam tended to slide along the cracked section at the base of the beam, and further displacement increase had no effect on the cracks along the beam and within the joint zone. Final failure of S4 was caused by the tensile rupture of reinforcement at the displacement of 7 Δ_y (Fig.7) with corresponding load of 109.2 kN. Compared with S2, S4 failed by full development of plastic hinge at the base of the beam.

Specimen S5 is a RC/ECC composite beam-column joint with two stirrups in the joint zone and constant axial load of 525 kN on the column during the loading process. For specimen S5, the deformation and cracking behaviors were very similar to that of specimen S4, while yielding of the specimen occurred at the load of 97.6 kN with corresponding displacement of 11.9 mm, which was smaller than that of S4. After yielding, the flexural cracks concentrated near the base of the beam where yielding of steel reinforcement occurred. Shear sliding occurred along the section of the beam base at the displacement of 7 Δ_y, and steel rupture occurred at the same section at the displacement of 7 Δ_y due to reversed horizontal loading. The failure load of specimen S5 was 106.7 kN with corresponding displacement of 84.5 mm. The failure mode of specimen S5 was the same as that of specimen S4, i.e. fully development of plastic hinge at the base of the beam for joint specimen. The crack pattern of specimen S5 is shown in Fig. 7.

Specimen S6 is a RC/ECC composite beam-column joint with three stirrups in the joint zone and a constant axial load of 350 kN on the column. The deformation and cracking behaviors of S6 were definitely similar to S4 and S5, while yielding of S6 occurred at the load of 96.5 kN with corresponding displacement of 13.3 mm. With increasing displacement loading, specimen S6 finally failed by rupture of reinforcement due to fully

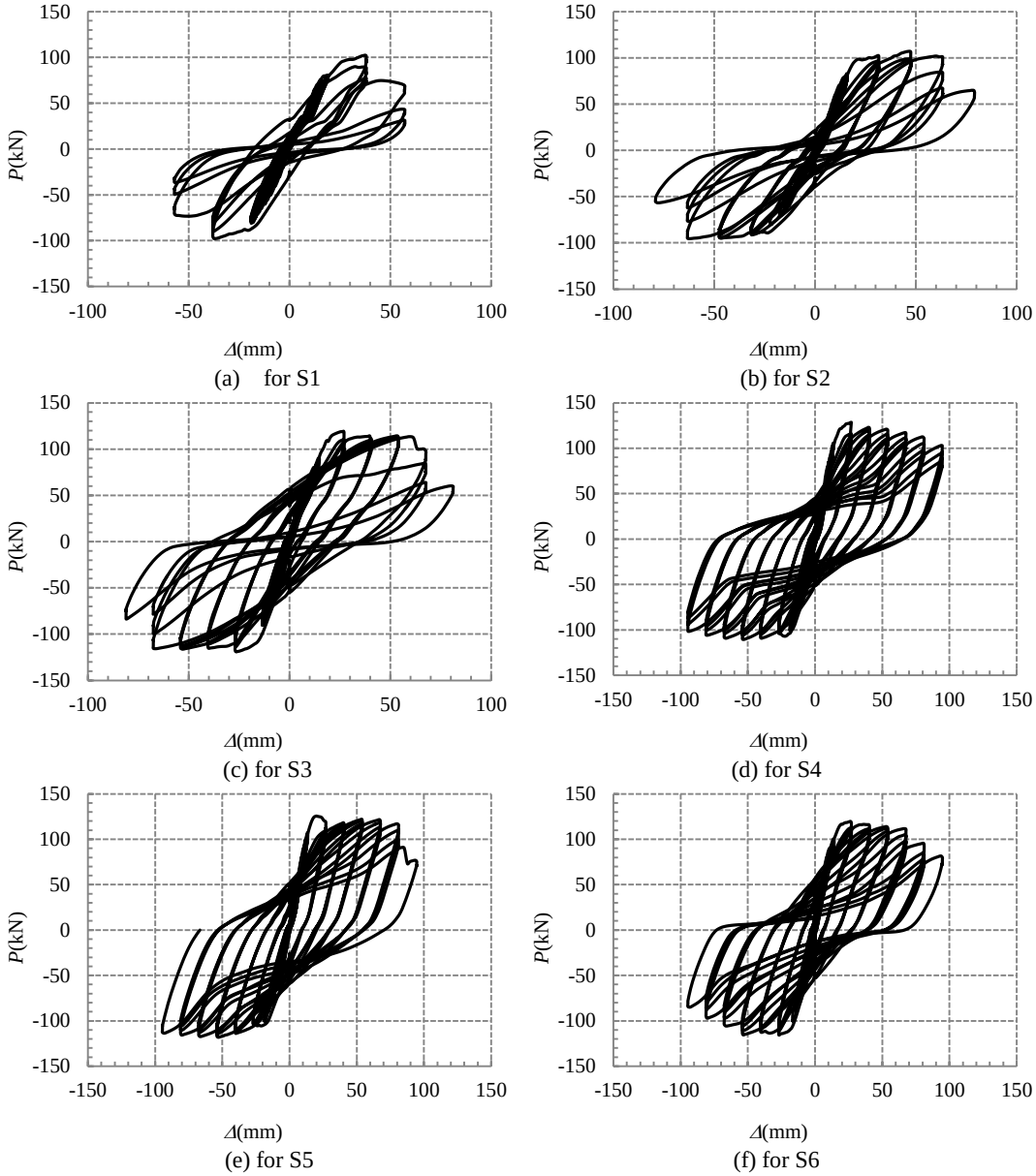

Fig 8: Cyclic load (P) versus lateral displacement (Δ) curves

development of the plastic hinge at the base of the beam (Fig. 7). The failure load and displacement were 101.7 kN and 74.6 mm respectively. The detailed test results for each specimen can be obtained in Table 1.

3.2 Load-displacement responses

Fig. 8 shows the curves of lateral load (P) versus lateral displacement (Δ) for each specimen. For specimen S1, the shear force in the joint zone was only undertaken by concrete and longitudinal steel reinforcement, leading to premature cracking of concrete under shear and compression stresses. When the lateral displacement reached 2 Δ_y, shear cracks opened significantly and spalling of concrete occurred, indicating final failure was reached. For specimen S1, pinching effect of hysteresis loops was apparent as shown in Fig. 8(a), indicating a brittle failure characteristic of specimen S1. Compared with S1, the hysteresis loops of S2 were relatively full and stable, and no apparent pinch effect was observed. This is due to the fact that application of steel stirrups in the connection zone enhanced the resistance to shear force

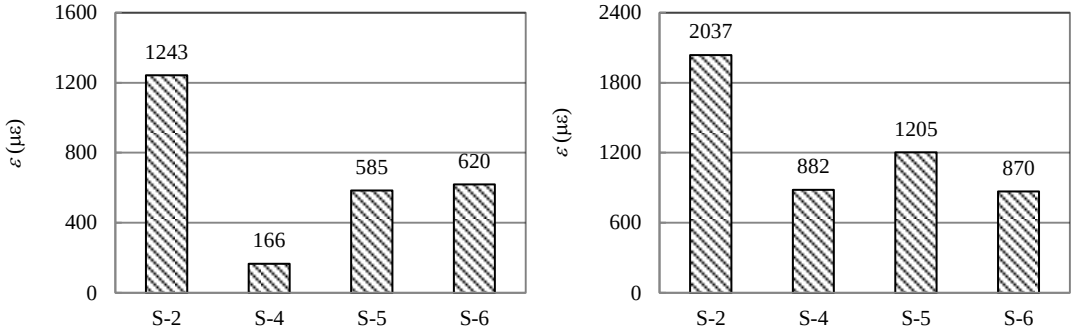

(a) at the yielding load (b) at the peak load

Fig 9: Strain values for each specimen

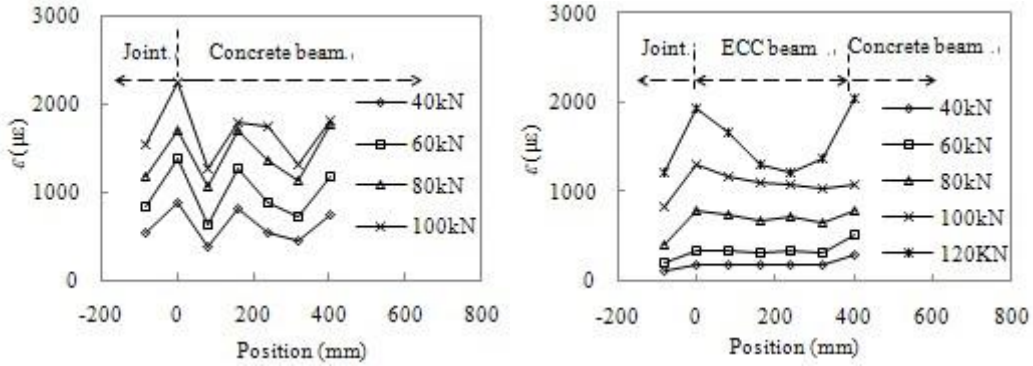

(a) for specimen S2 (b) for specimen S4

Fig 10: The strain distributions along the longitudinal steel reinforcement

and provided confinement of concrete core, resulting in higher compressive strength of concrete.

ECC is a kind of composite material with superior high ductility and damage tolerance, and deforms compatibly with steel reinforcement due to the same tensile properties. For steel reinforced ECC member, bond splitting or ECC spalling can be avoided under external loading, which can also be observed from the test results of specimen S3. Meanwhile, ECC had much better shear strength than normal concrete with the same compressive strength [8]. For the specimens without stirrups in the joint zone, specimen S3 showed much higher load capacity and ductility than specimen S1, although they failed in the same failure mode, i.e. brittle shear failure in the joint zone. According to Fig. 8, the area within the hysteresis loops of S3 was much higher than that of S1 and S2, indicating that substitution of ECC in the joint zone can significantly increase the energy dissipation ability under reversed cyclic loading. Even compared with specimen S2 which had two stirrups in the joint zone, the ultimate load capacity of specimen S3 is 11.4% higher than that of S2, which means that application of ECC in the joint zone can improve the shear strength significantly and even can substitute the steel stirrups with the same structural performance.

Compared with specimen S2, the ultimate load capacity of specimen S4 is 16.7% higher than that of S2 due to the dual enhancement from ECC and stirrups in the joint zone. For specimen S2 and S4, the failure mode also transferred from the shear failure in the joint zone to flexural failure at the base of the beam with full development of plastic hinge. For specimen S5 and S6, increase of the axial load in the column and addition of three stirrups within the joint zone seemed to have little effect on the seismic behavior of specimens, which may be due to that they both failed by flexural failure at the base of the beam. The

hysteresis loops of specimens S-5 and S-6 were generally similar to those of specimen S3 and S4.

3.3 Strain analysis

For each specimen, the strain variations in the stirrups have been collected during the loading process. Fig. 9 shows the maximum strains of the stirrups in the joint zone at the yield load and peak load. When the specimens reached yielding load, the maximum strain in the stirrups of specimen S2 is 1243 με, which is much larger than that of the other three RC/ECC composite joint specimens due to wide opening of shear cracks in RC joint.In the ultimate stage, the strain in the stirrups of specimen S2 is 2037 με, which is beyond the yielding strain (1800 με) and is more than two times of the other three specimens. It is attributed to the fact that the crack width in joint of RC specimen (S2) is much larger than that of specimens S4, S5 and S6, in which the fibers have bridged and restrained the cracks.

To analyze the strains distributions along the longitudinal reinforcement, the results of specimen S2 and S4 are used for examples. Fig. 10 shows the strain distributions along the longitudinal reinforcement of specimen S2 and S4 at different load levels. For specimen S2, the premature flexural cracks occurred along the RC beam, which led to the fluctuated distribution of strains along the longitudinal reinforcement in the beam. In contrast, for specimen S4, the strains along the longitudinal reinforcement in the beam distribute uniformly until the load increased to 100 kN due to opening of multiple and tiny cracks along the beam. In this stage, the longitudinal steel reinforcement had compatible deformation with ECC material and showed good bond with ECC. For each load value, the strains along the longitudinal reinforcement in specimen S4 are much smaller than those in specimen S2 due to strain hardening of ECC and compatible deformation between ECC and longitudinal steel reinforcement.

3.4 Ductility and energy dissipation

The ductility coefficient (μ) is an important parameter for evaluating the ductility performance of beam-column joints. The ductility coefficient (μ) is defined as Δ_u/Δ_y, where Δ_y is the lateral displacement at yield load and Δ_u is the displacement when the applied load declines to 85% of the maximum load. The value of μ for each specimen is listed in Table 1. For specimens without stirrups in the joint zone, the ductility coefficient of S3 is 1.61 times of that of S1, which is due to substitution of concrete with ECC in the joint zone. For the specimens with stirrups in the joint zone, the ductility coefficients of S4, S5 and S6 are 1.47, 1.67 and 1.32 times of that of S2. The enhanced shear strength and confinement effect of ECC are responsible for the improvement of ductility coefficient of RC/ECC composite joint specimens. The ductility coefficient of specimen S5 is larger than S4, which is due to the fact that improvement of axial load on the column contributed to restrain propagation of cracks in the joint zone and near the base of the beam. Redundant amount of stirrup may lead to difficulties in arranging transversal reinforcement and proper placement of concrete in the joint zone. That is why the ductility coefficient of specimen S6 is smaller than that of specimen S4.

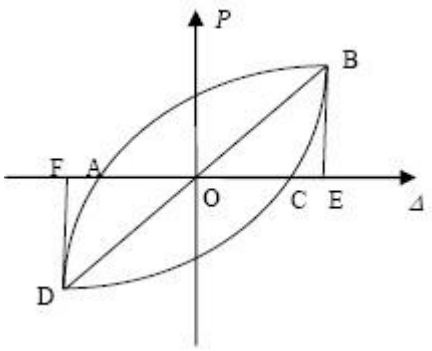

Fig 11: Hysteresis loop and energy dissipation

Equivalent damping coefficient (ξ_{eq}) is another important parameter for evaluating the energy dissipation capacity of beam-column joint specimens. Equivalent damping coefficient (ξ_{eq}) can be calculated according to the hysteresis loops in Fig. 11, and can be expressed as:

$$\xi_{eq} = \frac{1}{2\pi} \frac{S_{ABC} + S_{CDA}}{S_{OBE} + S_{ODF}} \quad (3)$$

where S_{ABC} and S_{CDA} are the areas enclosed by the curves ABC and CDA respectively, which denote the inelastic dissipating energy in one complete hysteresis loop. Similar definitions were used for S_{OBE} and S_{ODF} which denote the inelastic strain energy at a given displacement amplitude.

For each specimen, the cumulative energy dissipation is defined as the sum of the areas of each hysteresis loop before the considered load level or displacement step. Fig. 12 and Fig.13 show the equivalent damping coefficient ξ_{eq}-Δ/Δ_y curves and cumulative energy dissipation-Δ/Δ_y curves for each specimen. Specimen S1 and S3 are the beam-column joint specimens without stirrups in the joint zone. Specimen S1 reached the ultimate load at displacement of 3 Δ_y, and showed little energy dissipation capacity beyond ultimate load due to brittle shear failure in the joint zone, while S3 showed steadily energy dissipation capacity after ultimate load and failed at the displacement of 64.2 mm, resulting from strain hardening property of ECC in the joint zone. The cumulative energy dissipation of S3 is 3.7 times of that of S1.

For specimens with stirrups in the joint zone, specimen S2 showed the same the equivalent damping and cumulative dissipated energy with S4 when the displacement was smaller than 4 Δ_y. After that, spalling of concrete occurred in the joint zone and the energy dissipation ability of S2 decreased sharply with further loading. While, specimen S4 showed steadily energy dissipation capacity until lateral displacement reached 7 Δ_y (83.8 mm), which is attributed to superior ductile behavior of ECC and the abundant inelastic deformation of steel reinforcement along with ECC. During the loading process, no spalling of ECC and no buckling of longitudinal steel reinforcement occurred in the joint zone. It is found that the cumulative dissipated energy of specimen S5 is larger than specimen S4, indicating that higher axial load on the column

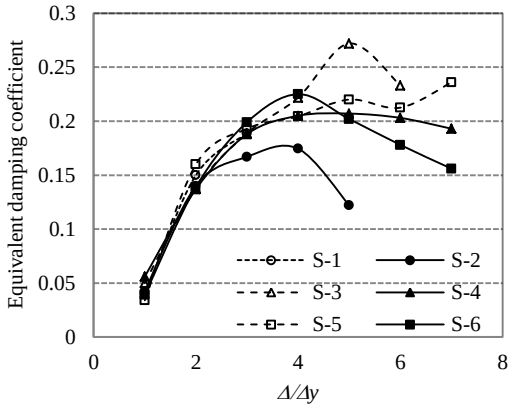

Fig 12: Equivalent damping coefficient ξeq-Δ/Δy curves of each specimen

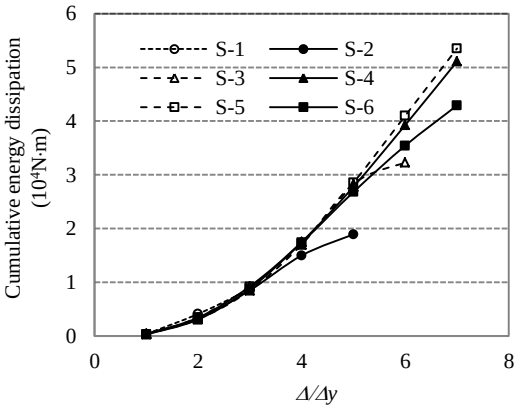

Fig 13: Cumulative energy dissipation-Δ/Δy curves of each specimen

is beneficial to prevent propagation of cracks in the joint zone and can lead to higher energy dissipation ability. For specimen S6, which had three stirrups in the joint zone, the energy dissipation capacity is little smaller than that of S4, which may be caused by the defects in the joint zone when concrete casting was conducted.

4 CONCLUSION

In the present paper, a number of beam-column joint specimens with different configurations have been tested to investigate the effect of ECC in the joint zone on the seismic behavior of the beam-column joint specimens. For the specimens without stirrups in the joint zone, addition of ECC in the joint zone can significantly increase the load capacity and ductility of the beam-column joint specimens, as well as the energy

dissipation due to high ductility and shear strength of ECC material. For the specimens with reduced or proper shear reinforcement in the joint zone, replacement of concrete with ECC in the joint zone can lead to failure mode change from brittle shear failure in the joint zone to flexural failure due to yielding of longitudinal steel reinforcement at the base of the beam. The RC/ECC composite beam-column joint showed higher load capacity, ductility and energy dissipation when compared with normal RC beam-column joint specimen. Increase of the axial load on the column cannot increase the ultimate load capacity and ductility since they all failed by flexural failure at the base of the beam, but can result in increased ductility coefficient because the additional axial load can restrain propagation of cracks in the joint specimen. Experimental results showed that increase of shear reinforcement in the joint zone may lead to difficulty in concrete casting, and the ultimate load capacity and ductility showed a small decrease with increasing the shear reinforcement ratio. In a word, substitution of concrete with ECC in the joint zone can significantly increase the seismic performance of beam-column joints even with decreased shear reinforcement in the joint zone compared with proper designed RC members.

ACKNOWLEDGEMENT

Financial support of the work by National Natural Science Foundation of China under 51278118, by the National Basic Research Program of China (973 Program) under 2009CB623200 and the Priority Academic Program Development of Jiangsu Higher Education Institutions, is gratefully acknowledged.

REFERENCES

[1] Ghobarah, A. and Said, A., 2002. Shear strengthening of beam-column joints. *Eng. Struct.* **24(7)**:881-888.

[2] Waston, S., Zahn, F. A., and Park, R., 1994. Confining reinforcement of concrete columns. *ACI. J. Struct. Eng.* **120(6)**:1798-1823.

[3] Kim, Y. Y., Fischer, G., and Li, V. C., 2004. Performance of bridge deck link slabs designed with ductile ECC. *ACI. Struct. J.* **101(6)**:792-801.

[4] Lepech, M. D., and Li, V. C., 2009. Application of ECC for bridge deck link slabs. *RILEM. J. Mater. Struct.* **42(9)**:1185-1195.

[5] Lepech, M. D., and Li, V. C., 2010. Sustainable pavement overlays using engineered cementitious composites. *J. Pavement. Res. Technol.* **3(5)**:241-250.

[6] Zhang, J., Leung, C. K. Y., and Gao, Y., 2009. Simulation of crack propagation of fiber reinforced cementitious composite under direct tension. *Eng. Fract. Mech.,* **78(12)**:2439-2454.

[7] Li, V. C., Mishra, D. K., and Wu, H. C., 1995. Matrix design for pseudo strain-hardening fiber reinforced cementitious composites. *RILEM. J. Mater. Struct.* **28(183)**:586-595.

[8] Li, V. C., and Mishra, D. K., 1996. Structural applications of engineered cementitious composites. *Indian. Concr. J.* **70(10)**:561-574.

[9] Fischer, G., and Li, V. C., 2002. Influence of matrix ductility on tension-stiffening behavior of steel reinforced engineered cementitious composites. *ACI. Struct. J.* **99(1)**:104-111.

[10] Li, V. C., and Wang, S., 2002. Flexural behaviors of glass fiber-reinforced polymer (GFRP) reinforced engineered cementitious composite beams. *ACI. Mater. J.* **99(1)**:11-21.

[11] Fisher, G., and Li, V. C., 2002. Effect of matrix ductility on deformation behavior of steel reinforced ECC flexural members under reversed cyclic loading condition. *ACI. Struct. J.* **99(6)**:781-790.

[12] Fisher, G., and Li, V. C., 2003. Intrinsic response control of moment resisting frames utilizing advanced composite materials and structural elements. *ACI. Struct. J.* **100(2)**:166-176.

[13] Cheung, Y. N., 2004. Investigation of concrete components with a pseudo-ductile layer. Doctoral thesis. Hong Kong University of Sci & Technol.